Biophysical Chemistry, 31 (1988) 269–274
Elsevier

BPC 01275

Acrylamide quenching of Y_t-base fluorescence in aqueous solution

Ignacy Gryczynski [a,*], Michael L. Johnson [b] and Joseph R. Lakowicz [a]

[a] *University of Maryland at Baltimore, School of Medicine, Department of Biological Chemistry, 660 West Redwood Street, Baltimore, MD 21201 and* [b] *University of Virginia School of Medicine, Department of Pharmacology, Charlottesville, VA 22908, U.S.A.*

Received 22 January 1988
Revised manuscript received 28 April 1988
Accepted 29 April 1988

Lifetime decay; Fluorescence quenching; Frequency-domain fluorometry; Transient effect

Acrylamide was found to be an effective quencher of Y_t-base (Y-4,9-dihydro-4,6-dimethyl-9-oxo-1*H*-imidazo-1,2*a*-purine) in water. In the absence of collisional quenching the decay of Y_t-base in water is predominantly a single exponential. The intensity decays become increasingly heterogeneous when quenched by acrylamide. The frequency-domain data were analyzed using the radiation model, which provides estimates of molecular parameters characteristic of the system. The mutual diffusion coefficient at 20 °C was found to be 0.5×10^5 cm^2/s, the Y_t-base acrylamide interaction radius was 8 Å, and the rate constant for quenching was 100 cm/s. These values indicate that quenching is diffusion-limited, i.e., the encounter complex is deactivated at least 2-fold faster than the rate of diffusive encounters.

1. Introduction

The Y_t-base,4,9-dihyro-4,6-dimethyl-9-oxo-1*H*-imidazo-1,2*a*-purine, is the simplest of the modified Y-like bases occurring in transfer ribonucleic acids specific to phenylalanine ($tRNA^{Phe}$). In recent years, several papers have been published [1–5] concerning the physicochemical properties of this modified nucleotide. It has been of special interest because of its strong fluorescence which offers a unique tool for probing the conformational properties of $tRNA^{Phe}$ [6,7] or more simple synthetic compounds such as Y_t-$(CH_2)_2$-adenine [8–10]. Recently we reported enhanced resolution of fluorescence anisotropy decays [11,12] and spectral relaxation [13] using progressively quenched samples. We now describe studies of acrylamide quenching of Y_t-base in aqueous solution. These studies reveal reaction rates and encounter radii, and also provide a test of the radiation model for collisional quenching [18,19]. Additionally, these measurements provide information needed for future studies of more complex Y_t-base-containing species, such as the dynamic and hydrodynamic properties of $tRNA^{Phe}$ or conformational distributions in the Y_t-$(CH_2)_n$-adenine and Y_t-$(CH_2)_3$-Y_t systems [14].

Correspondence address: J.R. Lakowicz, University of Maryland at Baltimore, School of Medicine, Department of Biological Chemistry, 660 West Redwood Street, Baltimore, MD 21201, U.S.A.

* Permanent address: Institute of Experimental Physics, University of Gdansk, Gdansk, Poland.

2. Materials and methods

The frequency-domain data were measured using a 2 GHz harmonic content fluorometer. The excitation wavelength was 310 nm from the frequency-doubled output of a R6G dye laser [15]. Magic angle polarizer orientations were used to eliminate the effects of rotational diffusion. The emission was observed through a Corning 0-52

band-pass filter, which absorbs all the emission and/or scattered light below 340 nm. The Y_t-base was prepared by reacting 3-methylguanine with bromoacetone [16,17], prior to these measurements being purified by HPLC. Acrylamide was from Biorad and had no absorption at 310 nm. All measurements were performed at 20 °C in 25 mM Tris buffer (pH 7).

3. Theory

3.1. Transient effect in quenching

The theory for transients in quenching is too complex to present in detail in this short report. Briefly, there are two practical models: the Smoluchowski ($\sqrt{t}$) model and radiation boundary condition (RBC) model [18–20]. A first model assumes that the fluorophore is quenched instantaneously when the quencher reaches a distance R from the fluorophore. A second, more complete model assumes that the fluorophore is quenched with a rate constant κ when at distance R from the quencher. The time-dependent rate constant for quenching is given by

$$k(t) = \frac{4\pi RDN'}{1 + D/\kappa R}\left[1 + \frac{\kappa R}{D}\exp(x^2)\,\mathrm{erfc}(x)\right] \quad (1)$$

where

$$x = \frac{\sqrt{Dt}}{R}\left[1 + \frac{\kappa R}{D}\right] \quad (2)$$

In this expression R denotes the interaction radius, D the sum of the diffusion coefficients of the fluorophore and quencher, $N' = 6.02 \times 10^{20}$ and κ is the specific rate constant for quenching in units of cm/s. The intensity decay is given by

$$I(t) = I_0 \exp\left(-\frac{t}{\tau_0}\right)\exp\left\{-[\mathrm{Q}]\int_{t=0}^{t} k(t)\,\mathrm{d}t\right\} \quad (3)$$

where [Q] is the molar quencher concentration.

3.2. Frequency-domain fluorometry

The intensity decays were examined in the frequency domain. The samples are excited with amplitude-modulated light, over the range of modulation frequencies from 10 to 1000 MHz. At each modulation frequency (ω), we measure the phase delay (ϕ_ω) and the extent of demodulation (m_ω), each relative to the incident light. The frequency response of the emission was analyzed using a sum of exponentials, and the more complex radiation model (eq. 3). For a sum of exponentials the intensity decay is described by

$$I(t) = \sum_i \alpha_i e^{-t/\tau_i} \quad (4)$$

The fractional contribution of each decay time to the steady-state intensity is

$$f_i = \frac{\alpha_i \tau_i}{\sum_i \alpha_i \tau_i} \quad (5)$$

For any form of the decay law the phase and modulation values are given by

$$\phi_\omega = \arctan(N_\omega / D_\omega) \quad (6)$$

$$m_\omega = \left(N_\omega^2 + D_\omega^2\right)^{1/2} \quad (7)$$

where

$$N_\omega = \int_0^\infty I(t)\sin\omega t\,\mathrm{d}t \Big/ \int_0^\infty I(t)\,\mathrm{d}t \quad (8)$$

$$D_\omega = \int_0^\infty I(t)\cos\omega t\,\mathrm{d}t \Big/ \int_0^\infty I(t)\,\mathrm{d}t \quad (9)$$

For multiexponential decays (eq. 4), we use analytical expressions for the transforms [21,22]. For the other decay law (eq. 3) numerical integration was used. In particular, we used an adaptive Newton-Cotes 9-point integration [23]. The term $f(x) = \exp(x^2)\,\mathrm{erfc}(x)$ was obtained during the iterations from a look-up table. Values of $f(x)$ for x values between those in the look-up table were obtained by using spline interpolation (for more details see ref. 24). The parameters describing the decay law are compared with the calculated (c) values ($\phi_{c\omega}$ and $m_{c\omega}$). The goodness-of-fit is characterized by

$$\chi_R^2 = \frac{1}{\nu}\sum_\omega\left[\frac{(\phi_\omega - \phi_{c\omega})}{\delta\phi}\right]^2 + \frac{1}{\nu}\sum_\omega\left[\frac{m_\omega - m_{cw}}{\delta m}\right]^2 \quad (10)$$

where ν is the number of degrees of freedom, and

$\delta\phi$ and δm the experimental uncertainties in the phase and modulation values, respectively. We used values of 0.2° and 0.005, respectively, which were found to be appropriate for our instrument and measurement techniques. The parameters were determined by a nonlinear least-squares method [21,22,27].

4. Results and discussion

4.1. Stern-Volmer plot for quenching

Quenching data are most frequently presented as Stern-Volmer plots, which is shown for acrylamide quenching of Y_t-base (fig. 1). Also shown are the emission spectra, which are decreased in amplitude but not altered in shape by quenching. The Stern-Volmer quenching constant was found to be 12 M^{-1}.

In addition, values are shown of τ_0/τ where τ is the best single-exponential fit to the frequency response. In this case, the Stern-Volmer plot shows substantial positive deviations, which are due to the increasing proportion of the decay occurring as a short-lived component. A more linear Stern-Volmer plot was found when the mean decay times were used ($\langle\tau\rangle = f_1\tau_1 + f_2\tau_2$). The $\langle\tau_0\rangle/\langle\tau\rangle$ ratios were then in good agreement with the intensity ratios. The positive deviations observed with the single-decay-time ratio illustrate the difficulties encountered when using single apparent decay times to describe complex intensity decays. In this case, the positive deviation in the Stern-Volmer plot is an artifact, resulting from the use of a single weighted parameter (τ) to describe a complex phenomenon.

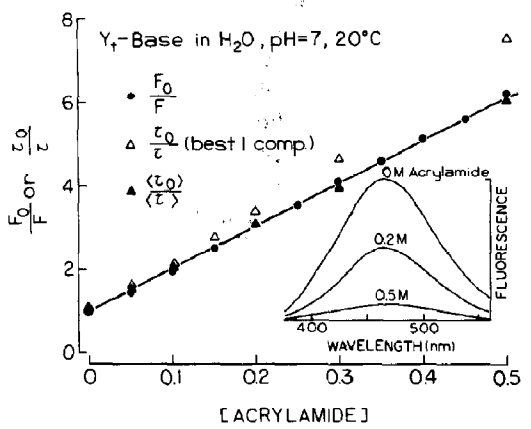

Fig. 1. Quenching of Y_t-base fluorescence by acrylamide at 20 °C. Stern-Volmer plots are shown for the yields (●), the mean decay time (▲) and the best single decay time (△). (Inset) Emission spectra in the presence of 0, 0.2 and 0.5 M acrylamide.

4.2. Nonexponential decays in the presence of quenching

The frequency-domain intensity decays of Y_t-base emission were measured with acrylamide concentrations ranging from 0 to 0.5 M (fig. 2). In the absence of quenching the emission from Y_t-base is dominately a single exponential, as can be seen from the agreement between the data (●), the best single-decay-time fit to the data (——, left), and the acceptable value of $\chi^2_R = 1.1$. In the presence of acrylamide (○) the frequency response

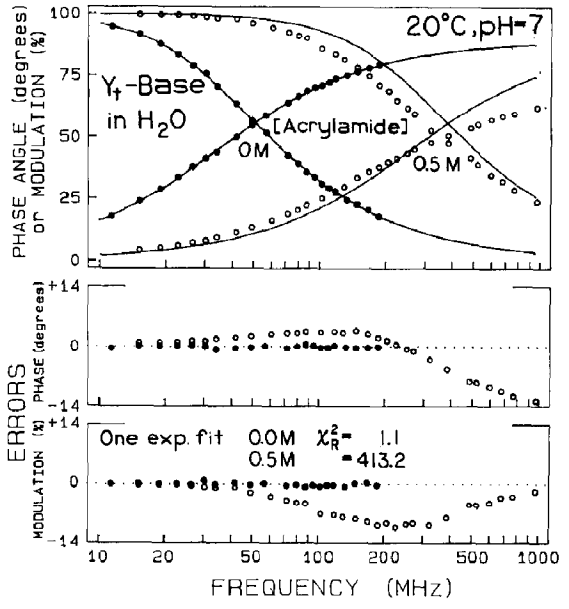

Fig. 2. Effect of acrylamide quenching on the intensity decay of Y_t-base. The solid lines represent the best single-decay-time fits to the data. Acrylamide concentrations: 0.0 (●) and 0.5 M (○). The lower panels show the deviations from the best single-decay-time fit.

shifts towards higher frequency, reflecting a decrease in the mean decay time of Y_t-base. Additionally, the intensity decay becomes extremely heterogeneous and can no longer be fitted by the single-decay-time model (——, right). This is also evident from the large and systematic deviations (lower panels) and the large value of χ^2_R.

The results from the multiexponential analysis over a range of acrylamide concentrations are summarized in table 1. In the absence of acrylamide there is no significant difference between the single- and double-exponential models. However, a significant degree of heterogeneity is already evident with merely 0.05 M acrylamide which resulted in a 35% decrease in the decay time. Even with this modest amount of quenching, the value of χ^2_R decreases 31-fold for the double-exponential model. The degree of heterogeneity increases progressively with increasing concentrations of acrylamide. At each acrylamide concentration the decay is characterized by a shorter and a longer decay time. Similar complex decays have been observed for the quenching of indole by acrylamide and iodide [24,27] and 1,2-benzanthracene by CCl_4 [20]. In general, the three-exponential decay analysis resulted in only a minor improvement in χ^2_R (not shown) and two of the three decay times were usually of similar magnitude.

Table 1

Acrylamide quenching of Y_t-base in water at 20 °C; multiexponential analysis

[Acrylamide]	τ (ns)	$\langle\tau\rangle$ (ns)	α_i	f_i	χ^2_R
0	4.64	–	1	1	1.2
	4.58	–	0.484	0.478	
	4.70	4.64	0.516	0.522	1.2
0.05	2.92	–	1	1	25.1
	0.68	–	0.128	0.031	
	3.12	3.04	0.872	0.969	0.8
0.1	2.05	–	1	1	74.9
	0.62	–	0.252	0.081	
	2.38	2.24	0.748	0.919	1.0
0.15	1.65	–	1	1	102.5
	0.31	–	0.298	0.064	
	1.91	1.81	0.702	0.936	2.2
0.2	1.36	–	1	1	187.8
	0.22	–	0.335	0.067	
	1.58	1.49	0.665	0.933	1.6
0.3	0.99	–	1	1	291.7
	0.25	–	0.432	0.125	
	1.32	1.18	0.568	0.875	2.1
0.5	0.62	–	1	1	412.8
	0.16	–	0.556	0.182	
	0.91	0.77	0.44	0.818	2.4

The good fits provided by the double-exponential model were noted previously for iodide and acrylamide quenching of indole [24]. However, it is important to bear in mind that the value of the decay times vary progressively with acrylamide concentration. This probably occurs because this model does not characterize the molecular features of the system, and the recovered values reflect some unspecified weighting of the data by the model.

4.3. Radiation model analysis

The radiation model is expected to provide a more realistic description because it contains appropriate molecular parameters, these being the interaction radius (R), mutual diffusion coefficient (D) and rate of deactivation of adjacent fluorophore-quenching pairs (κ). The results of this analysis are summarized in table 2, and one particular analysis is shown in fig. 3. In this case, the frequency responses measured at four acrylamide concentrations were analyzed simultaneously. Because of correlation among the parameters it is sometimes difficult to recover R, D and κ during the same least-squares analysis. Hence, we searched for a reasonable value of R, the interaction radius, by examination of the χ^2_R surface as R was held at fixed values. The minimum value of χ^2_R was found for $R = 8$ Å (fig. 4), and this value was used in all subsequent analyses. The radiation model with $R = 8$ Å yields good fits to the data (fig. 3), and essentially the same values of D and κ for all acrylamide concentrations (table 2).

The value of the diffusion coefficient, approx. 5×10^{-6} cm^2/s, is comparable to that determined previously for acrylamide quenching of indole. This value appears to be lower than expected,

Table 2

Radiation boundary model analysis of Y_t-base quenching in water at 20 °C [a]

[Acrylamide]	$D(\times 10^6)$ (cm^2/s)	κ (cm/s)	χ^2_R
0.05	4.87	114.7	0.8
0.1	4.77	114.5	1.3
0.15	4.33	105.2	3.2
0.2	4.74	95.2	3.0
0.3	3.61	90.9	1.4
0.5	3.13	84.4	2.1
0–0.1 [b]	4.81	114.4	1.0
0–0.15	4.79	107.0	6.9
0–0.2	4.98	99.9	11.4
0–0.3	5.13	91.9	26.5
0–0.5	5.25	85.9	44.0

[a] The interaction radius R was held constant at 8 Å. This means there are two variable parameters, D and κ. The value of τ_0 (from the fluorophore without quencher) is held fixed at the measured value.

[b] Global analysis of the data over the indicated range of acrylamide concentrations.

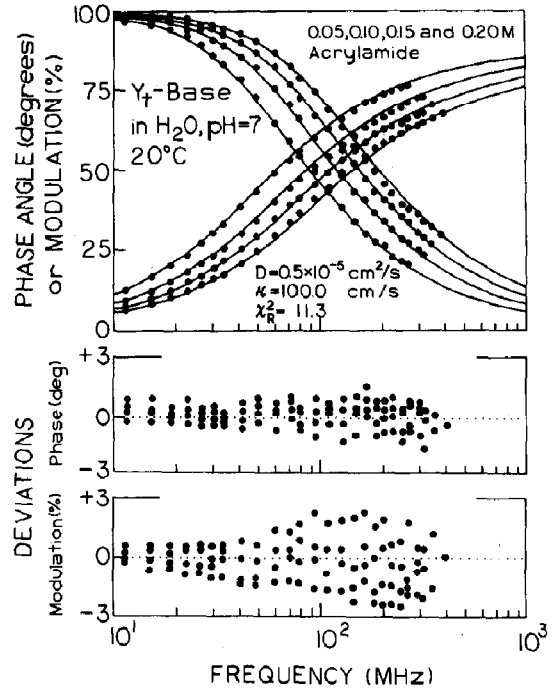

Fig. 3. Global RBC model analysis of the Y_t-base intensity decays in the presence of 0.05, 0.1, 0.15 and 0.20 M acrylamide. The data were analyzed using the radiation model with $R = 8$ Å. The lower panels show the deviations.

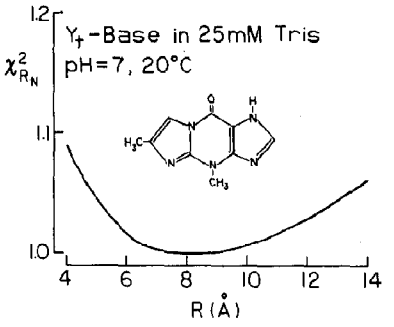

Fig. 4. Dependence of χ^2_R on the interaction radius R of Y_t-base and acrylamide for simultaneous analysis; 0–0.2 M acrylamide.

based on the diffusion coefficients of propanol or acetamide in water of approx. 1×10^{-5} cm^2/s [29,30]. However, the discrepancy is modest and probably within the uncertainties of our results and those resulting from the comparisons of non-identical molecules.

The value of κ is of interest because it indicates the rate of quenching of the Y_t-base–acrylamide encounter complex. The units of cm/s can be converted to the more familiar units for a bimolecular rate constant (M^{-1} s^{-1}) by calculating $k_q = \kappa 4\pi R^2 N'$, where $N' = 6.02 \times 10^{20}$. Using $R = 8$ Å and $\kappa = 100$ one obtains a quenching rate of 4.8×10^9 M^{-1} s^{-1}. This value is higher than that calculated from the slope of the Stern-Volmer plot. Using $k_q = K_D/\tau_0$ we calculate a biomolecular quenching constant of 2.6×10^9 M^{-1} s^{-1}. The greater value of k_q indicates that the quenching is indeed limited by diffusion. That is, the encounter complexes return to the ground state faster than they are formed by diffusion. At present, we believe that our data only define the lower limit for κ. It appears possible that the value of κ is larger, but that the measurements are not sensitive to values of κ which are much greater than the diffusion-limited quenching rate. From similar experiments on other fluorophore-quencher pairs we know that inefficient quenching results in lower values of κ (J.R. Lakowicz, I. Gryczynski, N. Joshi and M.L. Johnson, unpublished observations). Finally, we also noted that the global analyses are less satisfactory when the acrylamide concentrations exceed 0.15 M (table 2). In contrast, the

individual fits are adequate up to 0.5 M acrylamide. A similar effect was observed for iodide and acrylamide quenching of indole [24] and for a number of other fluorophore-quencher pairs (J.R. Lakowicz, I. Gryczynski, N. Joshi and M.L. Johnson, unpublished observations). In all cases, this failure is observed dominately for the global analyses of data ranging to quencher concentrations of 0.2 M or above. These other systems included the use of more symmetric quenchers like CCl_4 and CBr_4, so that the failure is probably not due to the asymmetric structures of Y_t-base or acrylamide. We suspect that the model fails at higher quencher concentrations because this concentration is treated in an approximate manner [18], which is only correct in the low concentration limit. To test this hypothesis we require a more exact solution of the radiation model, one which is correct for all concentrations of quencher. To the best of our knowledge, this solution has not yet appeared in the literature.

Acknowledgements

This work was supported by grant GM-39617 from the National Institutes of Health and grants DMB-8502835 and DMB-8511065 from the National Science Foundation. The authors thank Dr. Stefan Paszyc (Adam Mickiewicz University, Poznan, Poland) for providing Y_t-base and Dr. W. Wiczk for HPLC analysis of Y_t-base. I.G. is the recipient of partial support from CPBP 01.06.2.01 (Poland).

References

1 J. Eisinger, B. Feuer and T. Yamane, Proc. Natl. Acad. Sci. U.S.A. 65 (1970) 638.
2 E.M. Evleth and D.A. Lerner, Photochem. Photobiol. 26 (1977) 103.
3 S. Paszyc and M. Rafalska, Nucleic Acids Res. 6 (1979) 385.
4 I. Gryczynski, C. Jung, A. Kawski, S. Paszyc and B. Skalski, Z. Naturforsch. 34a (1979) 172.
5 I. Gryczynski, Z. Gryczynski, A. Kawski and S. Paszyc, Photochem. Photobiol. 39 (1984) 319.
6 W.E. Blumberg, R.E. Dale, J. Eisinger and D.M. Zuckerman, Biopolymers 13 (1974) 1607.
7 B.D. Wells and J.R. Lakowicz, Biophys. Chem. 26 (1987) 39.
8 I. Gryczynski, A. Kawski, S. Paszyc and B. Skalski, J. Photochem. 20 (1982) 71.
9 I. Gryczynski, A. Kawski, S. Paszyc and B. Skalski, Z. Naturforsch. 35a (1980) 1265.
10 I. Gryczynski, A. Kawski, S. Paszyc, B. Skalski and A. Tempczyk, J. Photochem. 30 (1985) 153.
11 J.R. Lakowicz, H. Cherek, I. Gryczynski, N. Joshi and M.L. Johnson, Biophys. J. 51 (1987) 755.
12 I. Gryczynski, H. Cherek, G. Laczko and J.R. Lakowicz, Chem. Phys. Lett. 135 (1987) 193.
13 J.R. Lakowicz, M. Szmacinski and I. Gryczynski, Photochem. Photobiol. 47 (1988) 31.
14 I. Gryczynski, A. Kawski, S. Paszyc, B. Skalski and A. Tempczyk, J. Photochem. (1988) submitted for publication.
15 J.R. Lakowicz, G. Laczko and I. Gryczynski, Rev. Sci. Instrum. 57 (1986) 2499.
16 H. Kasai, M. Goto, K. Iheda, M. Zama, Y. Mizuno, S. Takemura, T. Sugimoto and T. Goto, Biochemistry 15 (1976) 838.
17 I. Gryczynski, A. Kawski, K. Nowaczyk, S. Paszyc and B. Skalski, Biophys. Biochem. Res. Commun. 98 (1981) 1070.
18 F.C. Collins and G.E. Kimball, J. Colloid Sci. 4 (1949) 425.
19 F.C. Collins, J. Colloid Sci. 5 (1950) 499.
20 N. Joshi, M.L. Johnson, I. Gryczynski and J.R. Lakowicz, Chem. Phys. Lett. 135 (1987) 200.
21 J.R. Lakowicz, E. Gratton, G. Laczko, H. Cherek and M. Limkeman, Biophys. J. 46 (1984) 463.
22 J.R. Lakowicz and B.P. Maliwal, Biophys. Chem. 21 (1985) 61.
23 G.E. Forsythe, M.A. Malcolm and C.B. Moler, Computer methods for mathematical computations (Prentice Hall, Englewood Cliffs, NJ, 1977).
24 J.R. Lakowicz, M.L. Johnson, I. Gryczynski, N. Joshi and G. Laczko, J. Phys. Chem. 91 (1987) 3277.
25 M.L. Johnson and S.G. Frasier, Methods Enzymol. 117 (1985) 301.
26 J.R. Lakowicz, E. Gratton, G. Laczko, H. Cherek and M. Limkeman, Biophys. J. 46 (1984) 463.
27 J.R. Lakowicz, M.L. Johnson, N. Joshi, I. Gryczynski and G. Laczko, Chem. Phys. Lett. 131 (1986) 343.
28 J.R. Lakowicz, N. Joshi, M.L. Johnson, M. Szmacinski and I. Gryczynski, J. Biol. Chem. 262 (1987) 10907.
29 International Critical Tables of Numerical Data, Physics, Chemistry and Technology, 1926–1930, Editor-in-Chief, E.W. Washburn (McGraw-Hill, New York, 1926–1930) p. 70.
30 Handbook of Chemistry and Physics (CRC, Boca Raton, FL, 1967) p.F-45.